

BUCKLING ANALYSIS OF THIN FUNCTIONALLY GRADED RECTANGULAR PLATES WITH TWO OPPOSITE EDGES SIMPLY SUPPORTED

S.M. Kazerouni

Department of Mechanical Engineering, Islamic Azad University, Branch of Khomeinishah, Isfahan, Iran, sm_kazerooni@yahoo.com

*A.R. Saidi * and M. Mohammadi*

Department of mechanical engineering, Shahid Bahonar University of Kerman, Kerman, Iran, saidi@mail.uk.ac.ir, m.mohammadi@graduate.uk.ac.ir

*Corresponding Author

(Received: November 21, 2009 – Accepted in Revised Form: May 20, 2010)

Abstract In this article, an exact analytical solution for thermal buckling analysis of thin functionally graded (FG) rectangular plates is presented. Based on the classical plate theory and using the principle of minimum total potential energy, the stability equations are obtained. Since the material properties in FG materials are functions of the coordinates (specially the thickness), the stability equations are coupled in terms of in-plane and out-of plane displacements. Introducing a new analytical method, the coupled stability equations are converted into independent equations. It is assumed that the plate is simply supported on two opposite edges and has arbitrary boundary conditions along the other edges, so the Levy solution is considered. Two types of thermal loads, uniform and non-linear temperature rise through the thickness are considered as the loading conditions. Finally, the effect of aspect ratio, thickness to side ratio, index of FGM and boundary conditions on the critical buckling temperature of FG rectangular plates are discussed in details.

Keywords Thermal buckling, Functionally graded, Levy solution, Rectangular plate

چکیده در این مقاله، حل دقیقی برای کمانش ورق‌های نازک ساخته شده از مواد هدفمند ارائه شده است. بر اساس تئوری کلاسیک ورق و با استفاده از اصل مینیمم انرژی پتانسیل، معادلات پایداری تعیین شده‌اند. از آنجاییکه خواص مواد هدفمند تابع مختصات می‌باشند، در معادلات پایداری بین مولفه‌های کشش-خمش وابستگی وجود دارد. به منظور حذف این وابستگی، روش تحلیلی جدیدی پیشنهاد شده است که معادلات وابسته را به معادلات مستقل تبدیل می‌کند. فرض شده است که ورق دارای شرایط مرزی تکیه‌گاه ساده در دو ضلع روبرو بوده و در دو لبه دیگر ترکیبی از شرایط مرزی مختلف را دارد. بنابراین از روش لوی برای حل استفاده شده است. شرایط پارگذاری شامل دو نوع توزیع دمای یکنواخت و غیر خطی در جهت ضخامت در نظر گرفته شده است. نهایتاً، تاثیر نسبت منظری و ضخامت ورق، اندیس ماده هدفمند و شرایط مرزی روی دمای بحرانی کمانش مورد بررسی قرار گرفته است.

1. INTRODUCTION

In recent years, as the result of development in materials science, new materials with special applications were introduced which has been studied by many researchers. Functionally graded materials (FGMs) are composite materials that their thermal and mechanical properties differ smoothly and continuously from one surface to the

other surface. FGMs are capable of carrying thermal loads as well as mechanical loads and they are commonly used in engineering structures such as beams, plates and shells. These materials were introduced for the first time by Japanese researchers in 1984 [1]. The FG plates are used in power station furnaces, spacecrafts, rocket engines and high temperature instruments. Commonly, the ceramic surface of the FG plate is exposed to high

temperature side and the metal surface is exposed to low temperature side.

Many models were suggested for buckling analysis of isotropic and FG plates. Thermal and mechanical buckling analysis of FG plates was investigated by many researchers where most of the analytical solutions were limited to simply supported ones [2-5]. Javaheri and Eslami studied the mechanical buckling of FG rectangular plate under in-plane compressive loads based on the classical plate theory [2]. They determined equilibrium and stability equations using the variational approach and obtained the closed form solution for a rectangular plate. Thermal buckling analysis of FG rectangular plate based on the classical plate theory was carried out by Javaheri and Eslami [3]. In this study, it was shown that the critical buckling temperature reduces as the index of FGM increases. Also, they studied the thermal buckling analysis of FG rectangular plates according to the higher order plate theory (HOPT) [4]. It was assumed that the boundary conditions are simply supported in all edges and the closed form solution for the critical buckling temperature was obtained. Thermal buckling analysis of FG rectangular plates with geometrical imperfections was investigated by Samsam shariat and Eslami [5]. The equilibrium, stability and compatibility equations of imperfect FG rectangular plates were derived using the classical plate theory for the case of fully simply supported boundary condition and different loading conditions were considered. Lanhe [6] studied the thermal buckling of simply supported moderately thick FG rectangular plates. Using the first order shear deformation plate theory, the closed form solution for the critical buckling temperature was obtained and reported that the critical buckling temperature difference for a functionally graded plate is increased when the plate aspect ratio or the thickness to span ratio increases and it is decreased when the power law index increases.

Wu et al. [7] investigated the post-buckling analysis of FG rectangular plates under thermal and mechanical loads based on the first order shear deformation plate theory. They used fast converging finite double Chebyshev polynomials for different boundary conditions and considered von-Karman nonlinear kinematics. The buckling of thick FG rectangular plates under mechanical and

thermal loads was represented by Shariat and Eslami [8]. They assumed that the non-homogeneous properties of FG plate vary linearly through the thickness. The equilibrium and stability equations were derived based on the third order shear deformation plate theory and the Navier solution was used as the solution method. Abrate in different studies [9,10] showed that the mechanical and thermal buckling loads, the natural frequencies of FG rectangular plates and the deflections are always proportional to those of homogeneous isotropic plates. Conclusions were based on the comparison of the available results and since there were no results in buckling of FG plates, this case was incomplete. A generalized analytical approach to the buckling of simply supported isotropic rectangular plates under arbitrary loads was represented by Liu and Pavlovic [11]. They used the exact solutions for the in-plane stresses and the adoption of double Fourier series for the buckled profiles which, together ensure that accurate results are obtained in Ritz energy technique. A two-dimensional higher order deformation theory was presented for the evaluation of displacements and stresses in simply supported FG rectangular plates subjected to the thermal and mechanical loads by Matsunaga [12,13]. Hosseini-Hashemi et al. [14] reported the exact solution for linear buckling of isotropic rectangular plates. They used the Mindlin plate theory to study the buckling of in-plane loaded isotropic rectangular plates with various boundary conditions and presented critical buckling loads versus different parameters. Mohammadi et al. [15] studied the buckling analysis of thin functionally graded rectangular plates subjected to different mechanical loads. The coupled stability equations were decoupled analytically and the equations were solved for a plate with two opposite edges simply supported. The boundary conditions along the other edges were considered as a combination of simply supported, clamped and free. They inferred that increasing the index of FGM decreases the critical buckling load. An approximate method for simulation of natural frequencies and buckling loads of thin rectangular isotropic plates was represented by Mirzaeifar et al. [16]. The first and second order derivatives of natural frequencies and buckling loads with respect to arbitrary boundary conditions of an isotropic

rectangular plate were used in their study. Saidi et al. [17] investigated the axisymmetric bending and buckling of perfect thick FG solid circular plates using the unconstrained third order shear deformation plate theory. Saidi and Jomehzadeh [18] presented an analytical approach for the bending-stretching analysis of linearly elastic FG plates with two opposite edges simply supported and suggested a new method for decoupling the equations.

Praveen and Reddy [19] investigated the response of functionally graded ceramic-metal plates by the plate finite element that accounts for the transverse shear strains, rotary inertia and moderately large rotations in the Von Karman sense. They presented numerical results for the deflection and stresses of functionally graded plates and discussed on the effect of imposed temperature field on the dynamic and static response of fgm plate. Woo and Meguid [20] studied the plates and shallow shells made of functionally graded materials and provided an analytical solution for the coupled large deflections. They assumed that the structures are subjected to transverse mechanical and thermal loads and material properties vary through the thickness according to the power law distribution of the volume fraction of the constituents. They investigated the influence of the material properties on the dimensionless deflection, stresses and bending moments.

As was reviewed, all of the previous analytical studies for the thermal buckling analysis of functionally graded plates were limited to the special case of simply supported ones.

In this paper, the exact analytical solution for buckling analysis of FG rectangular plates subjected to the thermal loads is presented. Based on the classical plate theory and using the principle of minimum total potential energy, the stability equations are obtained for a rectangular plate. Applying an analytical method and introducing new functions, the stability equations are decoupled. Using Levy solution, the decoupled equations are solved analytically for a FG rectangular plate with two opposite simply supported edges. Finally, the thermal buckling analysis of FG rectangular plate subjected to two types of thermal loading has been investigated and the critical buckling temperatures for a FG

rectangular plate with different boundary conditions, various aspect ratios and thickness to side ratios and some index of FGM are presented in tables and figures.

The novelty of present work is to decouple the stability equations of FG rectangular plate by introducing new analytical method and obtaining the buckling temperature for thin FG plates with Levy boundary condition for the first time.

2. MATERIAL PROPERTIES

FGMs are usually composed of two parts, ceramic and metal where the properties vary by changing the volume fraction of these components. It is assumed that the material properties of FG plate vary through the thickness according to the power law function, as follow [19]

$$P(z) = P_m + P_{cm}(1/2 + z/h)^k, P_{cm} = P_c - P_m \quad (1)$$

where P denotes the material properties of FG plate such as modulus of elasticity (E), the coefficient of thermal expansion (α) and the thermal conductivity (K). The subscripts m and c refer to the metal and ceramic, respectively and the parameter k is known as the index of FGM. Also, h is the thickness of plate and z is the coordinate in the thickness direction. Since the variation of Poisson ratio through the thickness is negligible [21], the Poisson ratio is considered constant.

3. STABILITY EQUATIONS

According to the classical plate theory, the components of displacement field are considered as [22]

$$\begin{aligned} u(x, y, z) &= u_0 - z \frac{\partial w}{\partial x} \\ v(x, y, z) &= v_0 - z \frac{\partial w}{\partial y} \\ w(x, y, z) &= w(x, y) \end{aligned} \quad (2)$$

where u_0 and v_0 are the mid-plane displacements in x and y directions, respectively and w is the transverse displacement which are function of x and y variables. According to this theory, the strain components in z direction are zero. Thus, by considering the Von-Karman hypothesis, non-linear strain components are expressed as

$$\begin{aligned}\varepsilon_{xx} &= u_{,x} + \frac{1}{2}w_{,x}^2 - zw_{,xx} \\ \varepsilon_{yy} &= v_{,y} + \frac{1}{2}w_{,y}^2 - zw_{,yy} \\ \gamma_{xy} &= 2\varepsilon_{xy} = u_{,y} + v_{,x} + w_{,x}w_{,y} - 2zw_{,xy}\end{aligned}\quad (3)$$

Using the constitutive equations, the stress components are written in terms of the strain components. Therefore, considering the thermal effects on the plate, the stress components are expressed as

$$\begin{aligned}\sigma_{xx} &= \frac{E(z)}{1-\nu^2}(\varepsilon_{xx} + \nu\varepsilon_{yy} - (1+\nu)\alpha(z)\Delta T) \\ \sigma_{yy} &= \frac{E(z)}{1-\nu^2}(\varepsilon_{yy} + \nu\varepsilon_{xx} - (1+\nu)\alpha(z)\Delta T) \\ \sigma_{xy} &= \frac{E(z)}{2(1+\nu)}\gamma_{xy}\end{aligned}\quad (4)$$

Using the principle of minimum total potential energy, the equilibrium equations of thin rectangular plate subjected to the thermal loads are obtained as

$$\begin{aligned}N_{xx,x} + N_{xy,y} &= 0 \\ N_{yy,y} + N_{xy,x} &= 0 \\ M_{xx,xx} + M_{yy,yy} + 2M_{xy,xy} + N_{xx}w_{,xx} \\ &+ 2N_{xy}w_{,xy} + N_{yy}w_{,yy} = 0\end{aligned}\quad (5)$$

In equations (5), the parameters N_i and M_i ($i = xx, yy, xy$) are the force and moment resultants which are defined as

$$\begin{aligned}(N_{xx}, N_{yy}, N_{xy}) &= \int_{-h/2}^{h/2} (\sigma_{xx}, \sigma_{yy}, \sigma_{xy}) dz \\ (M_{xx}, M_{yy}, M_{xy}) &= \int_{-h/2}^{h/2} (\sigma_{xx}, \sigma_{yy}, \sigma_{xy}) z dz\end{aligned}\quad (6)$$

Since the strain components are non-linear in term of transverse displacement, the force and moment resultants and therefore the governing equilibrium equations are non-linear. To study the pre-buckling state, the linear equations are used which are obtained using the adjacent equilibrium criterion [22]. According to this criterion, it is assumed that the displacement components are consist of two states, equilibrium state and neighboring of this state which is presented by increments in displacement field. Therefore

$$\begin{aligned}u &= u^0 + u^1 \\ v &= v^0 + v^1 \\ w &= w^0 + w^1\end{aligned}\quad (7)$$

In equation (7), superscript 0 refers to the equilibrium and superscript 1 refers to the increment in the neighboring of this state.

Due to replacing equations (7) in the strain relations and the results in equations (6), the corresponding force and moment resultants are expressed as

$$\begin{aligned}N_i &= N_i^0 + N_i^1 \\ M_i &= M_i^0 + M_i^1\end{aligned}\quad (8)$$

where the terms with superscript 0 are related to the equilibrium state which contain the non-linear terms and satisfies the equilibrium equations and terms with superscript 1 are related to the neighboring state of equilibrium which contain the linear terms. So, the stability equations are obtained as

$$\begin{aligned}N_{xx,x}^1 + N_{xy,y}^1 &= 0 \\ N_{yy,y}^1 + N_{xy,x}^1 &= 0 \\ M_{xx,xx}^1 + M_{yy,yy}^1 + 2M_{xy,xy}^1 + N_{yy}^0 w_{,yy}^1 \\ &+ 2N_{xy}^0 w_{,xy}^1 + N_{xx}^0 w_{,xx}^1 = 0\end{aligned}\quad (9)$$

Substitution of the force and moment resultants in terms of displacement components and the results in the stability equations (9) yields in the following form of governing stability equations

$$\begin{aligned}
& E_1(u_{,xx}^1 + v_{,xy}^1) - E_2(w_{,xxx}^1 + w_{,yyy}^1) \\
& \quad + \frac{E_1(1-\nu)}{2}(u_{,yy}^1 - v_{,xy}^1) = 0 \\
& E_1(v_{,yy}^1 + u_{,xy}^1) - E_2(w_{,yyy}^1 + w_{,xxy}^1) \\
& \quad + \frac{E_1(1-\nu)}{2}(v_{,xx}^1 - u_{,xy}^1) = 0 \\
& E_2(u_{,xxx}^1 + u_{,xyy}^1 + v_{,yyy}^1 + v_{,xxy}^1) - E_3\nabla^4 w^1 \\
& \quad + N_x^0 w_{,xx} + 2N_{xy}^0 w_{,xy}^1 + N_y^0 w_{,yy} = 0
\end{aligned} \tag{10}$$

where the constants E_i are related to the material properties which are obtained by integrating of properties over the thickness and are expressed as follow

$$\begin{aligned}
E_1 &= \frac{E_m h}{1-\nu^2} + \frac{E_{cm} h}{(1-\nu^2)(k+1)} \\
E_2 &= \frac{E_{cm} h^2 k}{2(1-\nu^2)(k+1)(k+2)} \\
E_3 &= \frac{E_m h^3}{12(1-\nu^2)} + \frac{E_{cm} h^3 (k^2 + k + 2)}{4(1-\nu^2)(k+1)(k+2)(k+3)}
\end{aligned} \tag{11}$$

It can be seen from equation (10) that the stability equations are coupled in terms of displacement components. In order to decouple these equations, two new functions are defined as

$$\begin{aligned}
\varphi_1 &= u_{,x}^1 + v_{,y}^1 \\
\varphi_2 &= u_{,y}^1 - v_{,x}^1
\end{aligned} \tag{12}$$

Substituting equations (12) into (10) yields

$$\begin{aligned}
& \frac{E_1}{1-\nu^2} \varphi_{1,x} - \frac{E_2}{1-\nu^2} (w_{,xxx}^1 + w_{,yyy}^1) \\
& \quad + \frac{E_1}{2(1+\nu)} \varphi_{2,y} = 0
\end{aligned} \tag{13a}$$

$$\begin{aligned}
& \frac{E_1}{1-\nu^2} \varphi_{1,y} - \frac{E_2}{1-\nu^2} (w_{,yyy}^1 + w_{,xxy}^1) \\
& \quad - \frac{E_1}{2(1+\nu)} \varphi_{2,x} = 0
\end{aligned} \tag{13b}$$

$$\begin{aligned}
& \frac{E_2}{1-\nu^2} \nabla^2 \varphi_1 - \frac{E_3}{1-\nu^2} \nabla^4 w^1 + N_{xx}^0 w_{,xx} \\
& \quad + 2N_{xy}^0 w_{,xy}^1 + N_{yy}^0 w_{,yy} = 0
\end{aligned} \tag{13c}$$

In the following, doing some mathematical calculations, the coupled stability equations are converted to independent equations. Adding the differentiation of equation (13a) with respect to x and equation (13b) with respect to y yields

$$\nabla^2 \varphi_1 = (E_2 / E_1) \nabla^4 w^1 \tag{14}$$

Also, by subtracting the differentiation of equation (13a) with respect to y and equation (13b) with respect to x , the following equation is obtained for the function φ_2 as

$$\nabla^2 \varphi_2 = 0 \tag{15}$$

Upon substituting equation (14) into equation (13c), an independent equation for the unknown w^1 is obtained as

$$-\bar{D} \nabla^4 w^1 + N_{xx}^0 w_{,xx} + 2N_{xy}^0 w_{,xy}^1 + N_{yy}^0 w_{,yy} = 0 \tag{16}$$

Equation (16) is the governing differential equation for the stability of thin FG rectangular plates which is the same as isotropic one if the isotropic flexural rigidity is replaced by the equivalent flexural rigidity of FGMs \bar{D} , where $\bar{D} = E_3 - (E_2^2 / E_1)$.

It is easy to show that the following expressions for the in-plane components of displacement field satisfy equations (14) and (15)

$$u^1 = (E_2 / E_1) w_{,x}^1 ; \quad v^1 = (E_2 / E_1) w_{,y}^1 \tag{17}$$

The above equations show that in FGMs the mid-plane does not coincide with the neutral surface. Therefore, relation (16) is the only equation that must be solved for the buckling of FG plates.

4. BOUNDARY CONDITIONS

As it was mentioned before, Levy boundary conditions are considered. So, the plate is simply supported in x direction and has a combination of simply supported, clamped or free along the other edges. In the following, the letters S , C and F refer to simply supported, clamped and free, respectively. The conditions for each case are

$$\text{Simply Supported} \quad w^1 = 0, M_y = 0 \quad (18a)$$

$$\text{Clamped} \quad w = 0, w_{,y}^1 = 0 \quad (18b)$$

$$\text{Free} \quad M_y = 0, V_y + N_y^0 w_{,y}^1 = 0 \quad (18c)$$

In the above equations, the parameters M_y and V_y are defined as

$$M_y = -D(w_{,y}^1 + \nu w_{,xx}^1) \quad (19)$$

$$V_y = -D(w_{,yyy}^1 + (2 - \nu)w_{,xxy}^1)$$

Imposing the above boundary conditions on the edges $y=0$ and $y=b$, a homogenous system of algebraic equations is obtained. Setting the determinant of the coefficient equal to zero, the characteristic equation is obtained. The solution of this equation leads to find the critical buckling temperature. The characteristic equations for the six types of boundary conditions are listed in the appendix A. In the following, the notations such as SFSC show the order of boundary conditions (e.g. SFSC represents a plate with free edge at $y=0$ and clamped edge at $y=b$).

5. THERMAL BUCKLING ANALYSIS

Consider a rectangular plate with the length a , width b , and thickness h , as shown in Fig. 1. It is assumed that the plate is subjected to thermal loads. So, the equilibrium resultant thermal forces are defined as

$$N_{xx}^0 = -N_T, N_{yy}^0 = -N_T, N_{xy}^0 = 0 \quad (20)$$

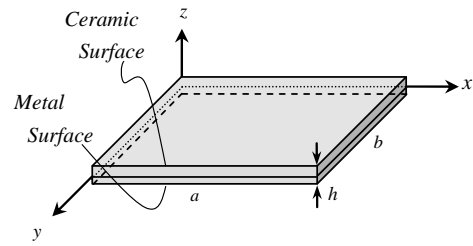


Figure 1. Geometry and coordinate system of a FG rectangular plate.

where N_T is pre buckling thermal force and is defined as

$$N_T = \int_{-h/2}^{+h/2} \frac{E(z)}{1-\nu} \alpha(z) \Delta T(z) dz \quad (21)$$

Substituting relations (20) into the stability equation (16) yields in

$$-\bar{D} \nabla^4 w^1 - N_T \nabla^2 w^1 = 0 \quad (22)$$

It is assumed that the plate is simply supported along two edges parallel to the y axis and has arbitrary boundary conditions along the other edges, so the Levy solution is considered as the solution method. Thus the Fourier series is considered for the transverse deflection function w^1 which satisfies the simply supported boundary conditions. Therefore

$$w^1 = \sum_{m=1}^{\infty} g(y) \sin(m\pi x/a) \quad (23)$$

Substituting equation (23) into equation (22), the following ordinary differential equation is obtained

$$-\bar{D} \frac{d^4 g}{dy^4} + \left(\bar{D} \left(\frac{m\pi}{a} \right)^2 - N_T \right) \frac{d^2 g}{dy^2} + \left(-\bar{D} \left(\frac{m\pi}{a} \right)^4 + N_T \left(\frac{m\pi}{a} \right)^2 \right) g = 0 \quad (24)$$

The solution of ordinary differential equation (24) is expressed as

$$g(y) = C_1 \cosh(\lambda_1 y) + C_2 \sinh(\lambda_1 y) + C_3 \cosh(\lambda_2 y) + C_4 \sinh(\lambda_2 y) \quad (25)$$

whereas the constants λ_1 and λ_2 are defined as

$$\lambda_1 = m\pi/a \text{ and } \lambda_2 = \sqrt{(m\pi/a)^2 - (N_T/D)} \quad (26)$$

Substituting equation (25) into the transverse deflection function (23) results in

$$w^1(x, y) = \sum_{m=1}^{\infty} (C_1 \cosh \lambda_1 y + C_2 \sinh \lambda_1 y + C_3 \cosh \lambda_2 y + C_4 \sinh \lambda_2 y) \sin\left(\frac{m\pi}{a} x\right) \quad (27)$$

where the parameters C_1 to C_4 are four unknown constants which are determined by satisfying the various boundary conditions. Two cases of thermal loadings, uniform and non-linear temperature rise through the thickness, are considered.

CASE I: UNIFORM TEMPERATURE RISE

In order to find the parameter N_T in equation (26) for the case of uniform temperature rise, it is assumed that the temperature is constant through the thickness. Let the initial temperature of plate be T_i and after thermal loading, temperature increases to the final value T_f , in which the plate buckles. The critical buckling temperature difference is defined as

$$\Delta T(z) = T_f - T_i = T_c \quad (28)$$

where $\Delta T(z) = T_c$ is a constant. Substituting equation (28) into equation (21), the resultant force corresponding to the thermal loading is obtained as

$$N_T = T_c \int_{-h/2}^{h/2} \frac{E(z)}{1-\nu} \alpha(z) dz \quad (29)$$

where T_c is the critical buckling temperature difference.

CASE II: NONLINEAR TEMPERATURE RISE ACROSS THE THICKNESS

Let the plate be at the initial temperature T_i . When the plate is subjected to thermal load, the temperature of ceramic side is increased to a final value T_c , while the temperature of metal surface is reached to the final value T_m .

In order to obtain the temperature gradient through the thickness $\Delta T(z)$, the one-dimensional Fourier steady state heat conduction equation is considered as follow

$$\frac{d}{dz} [K(z) \frac{dT}{dz}] = 0 \quad (30)$$

where $K(z)$ is the thermal conduction coefficient which vary according to the power law function as mentioned in equation (1). The thermal boundary conditions are

$$\begin{aligned} T(z) &= T_c \text{ at } z = h/2 \\ T(z) &= T_m \text{ at } z = -h/2 \end{aligned} \quad (31)$$

Solving equation (30) and imposing the boundary conditions (31), the temperature distribution function is obtained as [20]

$$T(z) = T_m + \frac{\left(\frac{2z+h}{2h}\right)^{cm} T_{cm} \sum_{n=0}^{\infty} \frac{\left(\frac{2z+h}{2h}\right)^k K_{cm}^n}{nk+1}}{\sum_{n=0}^{\infty} \frac{\left(-\frac{K_{cm}}{K_m}\right)^n}{nk+1}} \quad (32)$$

In the above equation, the subscript cm shows the differences of the corresponding parameters of ceramic and metal. Also, the temperature difference is defined as

$$\Delta T(z) = T(z) - T_i \quad (33)$$

Equation (32) is the exact solution for the one dimensional temperature distribution for FGMs.

Table 1. Comparison of the critical buckling temperature for a FG plate subjected to non-linear temperature rise for simply supported plate.

k		$a/b=1$	$a/b=2$	$a/b=3$	$a/b=4$	$a/b=5$
0	Ref. [3]	24.19821	75.4955	160.9911	280.6848	434.5768
	Ref. [6]	24.16215	75.3952	160.5901	279.5281	431.8769
	Present	24.1982	75.4955	160.9911	280.6848	434.5767
1	Ref. [3]	7.6635	38.6838	90.3842	162.7649	255.8257
	Ref. [6]	7.6554	38.6328	90.1801	162.1757	254.4500
	Present	7.6636	38.6838	90.3843	162.7649	255.8257
5	Ref. [3]	4.8774	28.3389	67.4414	122.1849	192.5694
	Ref. [6]	4.8699	28.2918	67.2531	122.6415	191.3010
	Present	4.8774	28.3389	67.4414	122.1849	192.3961

Substituting equation (33) into equation (19) gives the pre-buckling resultant force for non-linear temperature rise through the thickness.

6. RESULTS AND DISSCUSION

In order to verify the method and validate the results, a comparison with the available results has been done. In table 1, the numerical results presented in references [3] and [6] have been compared with the present results.

The results in Ref. [3] are presented for thin plates, but in Ref. [6], the results are obtained based on the first order shear deformation plate theory. In the comparison, the thickness to side ratio h/a is assumed to be 0.01 and $\Delta T_m = 5^\circ$. As the table shows, there is a good agreement between the obtained results and the available results in references.

To obtain the numerical results, it is assumed that the plate is made of Alumina as the ceramic part and Aluminum as the metal part with the following properties

Aluminum properties: $\alpha_m = 23 \times 10^{-6} (1/^\circ C)$

$E_m = 70 \text{ GPa}, K_m = 204 \text{ W/mK}$

Alumina properties: $\alpha_c = 7.4 \times 10^{-6} (1/^\circ C)$

$E_c = 380 \text{ GPa}, K_c = 10.4 \text{ W/mK}$

Also, it is assumed that the Poisson ratio is a constant and equal to 0.3. The critical buckling temperatures of FG rectangular plate are computed for both, the uniform and non-linear temperature rise cases.

In Fig. 2, the effect of index of FGM on the critical buckling temperature is shown for a plate with aspect ratio 2 and thickness to side 0.02.

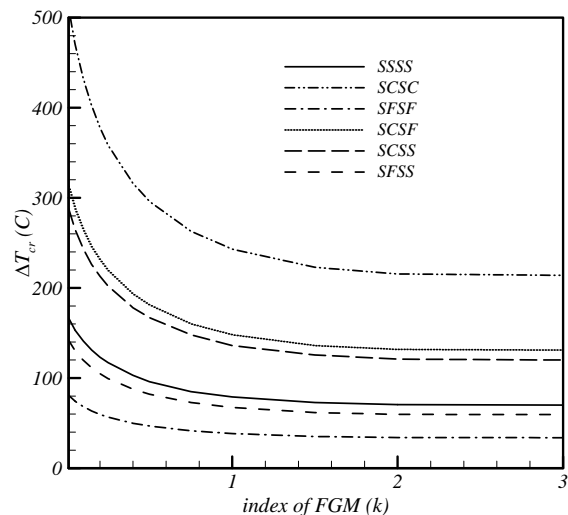


Figure 2. The critical buckling temperature versus the index of FGM ($a/b = 2, h/a = 0.02$).

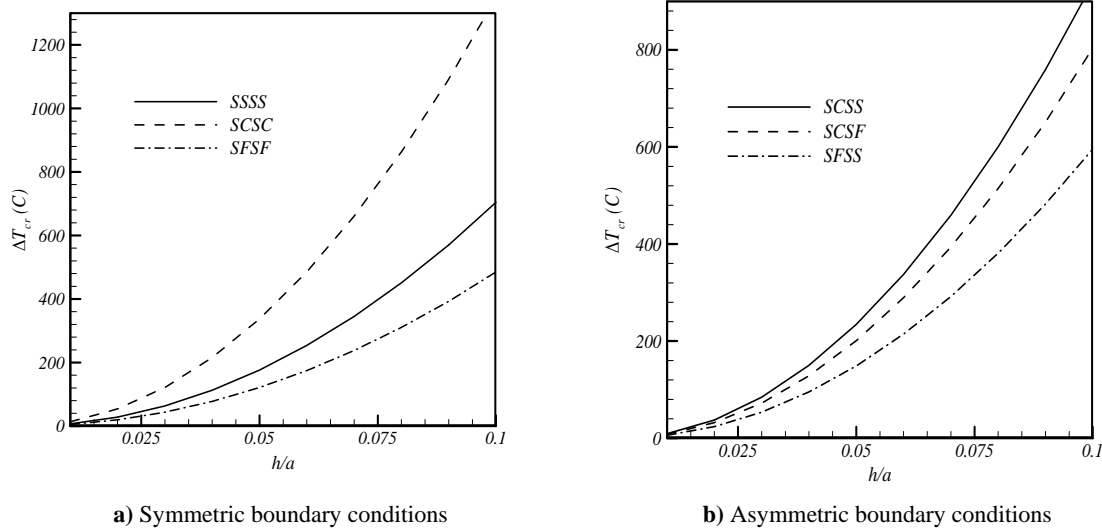


Figure 3. The effect of thickness to side ratio on the critical buckling temperature (under uniform temperature rise) for square FG plate with a) Symmetric boundary conditions, b) Asymmetric boundary conditions ($k = 2$).

Also, the influence of boundary conditions on the critical temperature is investigated within this figure. According to this figure, increasing the index of FGM decreases the critical buckling temperature. This is due to the higher index of FGM which corresponds to the higher portion of metal part in the material. Also, variation of ΔT_{cr} is more apparent for the smaller index of FGM. Since the SCSC plate is more constrained, the highest temperature refers to this case. In figures 3 and 4, the critical buckling temperature is plotted versus the thickness to side ratio.

According to these figures, increasing the thickness to side ratio (h/a) increases the critical temperature. Also, in all of the cases, the thermal loading capacity for the non-linear case is more than the uniform temperature case.

In tables 2 to 5, the critical buckling temperatures for plates with different aspect ratios, various indexes of FGM and symmetric and asymmetric boundary conditions are presented. It can be seen that, increasing the aspect ratio causes increasing the critical buckling mode. Moreover, the boundary condition has a significant effect on the variation of buckling mode.

7. CONCLUSION

In this paper, an exact analytical solution for thermal buckling analysis of functionally graded rectangular plates based on the classical plate theory has been presented. In order to decouple the stability equations, a new analytical method has been presented.

This method has been developed for a plate with two opposite edges simply supported and arbitrary boundary conditions along the other edges. The independent equations were solved analytically.

Finally, the critical buckling temperatures for FG plates with different boundary conditions, some aspect ratios and various index of FGM have been presented in figures and tables. So, it is concluded that the critical buckling temperature decreases as the index of FGM increases and increasing the thickness, increases the critical temperature.

As the results show, changing the aspect ratio and/or boundary condition change the buckling mode. Also, plates subjected to the non-linear temperature rise buckle at high temperature in comparison with those which are under uniform temperature rise.

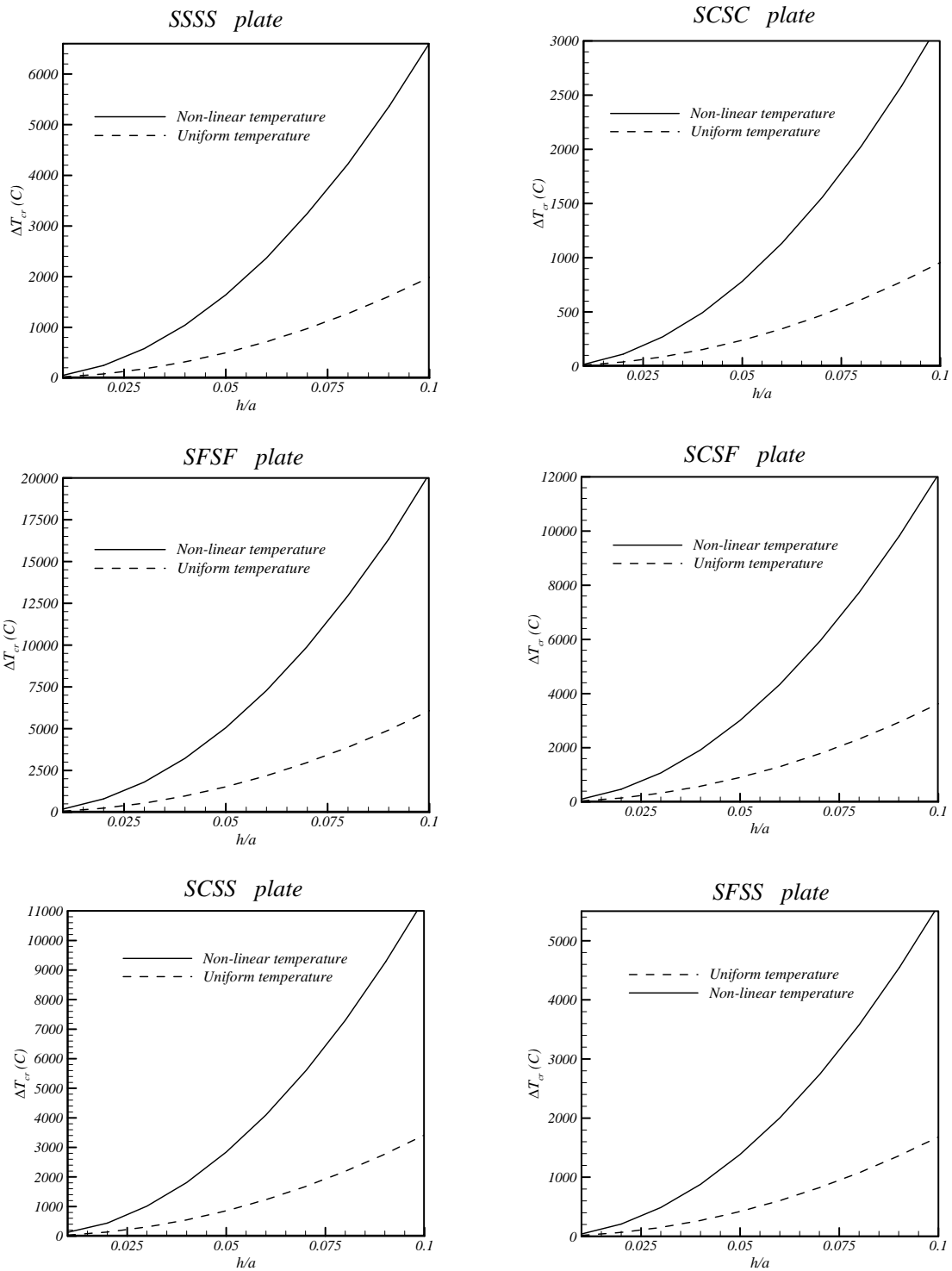


Figure 4. Comparison of the critical buckling temperature for square FG plate with different boundary conditions ($a/b = 2, k = 1$).

Table 2. The critical buckling temperature for a FG rectangular plate subjected to uniform temperature rise with symmetric boundary conditions.

Boundary conditions	k	$a/b = 1$	$a/b = 2$	$a/b = 3$	$a/b = 4$	$a/b = 5$
SCSC	0	32.74	130.79	289.90 ⁽²⁾	513.97 ⁽³⁾	809.12 ⁽⁴⁾
	0.5	18.55	74.11	164.25 ⁽²⁾	291.20 ⁽³⁾	458.42 ⁽⁴⁾
	1	15.21	60.76	134.68 ⁽²⁾	238.78 ⁽³⁾	373.22 ⁽⁴⁾
	2	13.49	53.87	119.40 ⁽²⁾	211.69 ⁽³⁾	313.25 ⁽⁴⁾
SFSF	0	11.78	20.62	35.31	55.88	82.31
	0.5	6.673	11.68	20.01	31.66	46.64
	1	5.472	9.578	16.40	25.96	38.24
	2	4.851	8.491	14.54	23.01	33.90
SSSS	0	17.09	42.45	85.49	145.34	222.29
	0.5	9.687	24.22	48.44	82.35	125.94
	1	7.944	19.86	39.72	67.52	103.27
	2	7.043	17.62	35.21	59.86	91.55

Numbers in parenthesis indicate the critical buckling mode.

Table 3. The critical buckling temperature for a FG rectangular plate subjected to uniform temperature rise with asymmetric boundary conditions.

Boundary conditions	k	$a/b = 1$	$a/b = 2$	$a/b = 3$	$a/b = 4$	$a/b = 5$
SCSF	0	19.52	79.97 ⁽²⁾	165.95 ⁽²⁾	291.97 ⁽³⁾	457.38 ⁽⁴⁾
	0.5	11.06	45.31 ⁽²⁾	94.02 ⁽²⁾	165.42 ⁽³⁾	259.14 ⁽⁴⁾
	1	9.07(1)	36.27 ⁽²⁾	77.09 ⁽²⁾	135.64 ⁽³⁾	212.49 ⁽⁴⁾
	2	8.039	32.94 ⁽²⁾	68.35 ⁽²⁾	120.25 ⁽³⁾	188.38 ⁽⁴⁾
SCSS	0	22.76	73.70	160.69	282.95	440.27
	0.5	12.89	41.76	91.05	160.31	249.45
	1	10.58	34.24	74.66	131.45	204.54
	2	9.381	30.36	66.19	116.54	181.33
SFSS	0	14.46	36.22	76.73	135.40	211.69
	0.5	8.193	20.52	43.47	67.72	119.94
	1	6.718	16.83	35.65	62.90	98.35
	2	5.956	14.92	31.60	55.77	87.19

Numbers in parenthesis indicate the critical buckling mode.

Table 4. The critical buckling temperature for a FG rectangular plate subjected to non-linear temperature rise with symmetric boundary conditions.

Boundary conditions	k	$a/b = 1$	$a/b = 2$	$a/b = 3$	$a/b = 4$	$a/b = 5$
SCSC	0	55.49	251.59	569.80 ⁽²⁾	1017.94 ⁽³⁾	1569.74 ⁽⁴⁾
	0.5	47.25	240.92	555.18 ⁽²⁾	997.77 ⁽³⁾	1569.39 ⁽⁴⁾
	1	34.08	186.08	432.73 ⁽²⁾	780.09 ⁽³⁾	1228.75 ⁽⁴⁾
	2	24.92	143.50	335.92 ⁽²⁾	606.90 ⁽³⁾	956.89 ⁽⁴⁾
SFSS	0	13.56	32.23	60.62	101.75	154.64
	0.5	5.835	23.29	52.31	92.93	145.15
	1	1.575	15.28	38.05	69.94	110.93
	2	0.013	10.25	28.02	52.89	84.86
SSSS	0	24.19	75.01	160.99	280.68	434.58
	0.5	16.34	67.01	151.85	269.65	421.64
	1	9.823	49.58	115.85	208.63	327.92
	2	5.99	37.02	88.71	161.09	254.15

Numbers in parenthesis indicate the critical buckling mode.

Table 5. The critical buckling temperature for a FG rectangular plate non-linear temperature rise with symmetric boundary conditions.

Boundary conditions	k	$a/b = 1$	$a/b = 2$	$a/b = 3$	$a/b = 4$	$a/b = 5$
SCSF	0	29.04	146.15 ⁽²⁾	321.91 ⁽²⁾	573.94 ⁽³⁾	904.77 ⁽⁴⁾
	0.5	21.12	136.77 ⁽²⁾	310.36 ⁽²⁾	559.27 ⁽³⁾	885.99 ⁽⁴⁾
	1	13.57	104.36 ⁽²⁾	240.58 ⁽²⁾	435.96 ⁽³⁾	692.37 ⁽⁴⁾
	2	8.92	79.74 ⁽²⁾	186.02 ⁽²⁾	334.42 ⁽³⁾	538.47 ⁽⁴⁾
SCSS	0	35.53	137.40	311.39	555.89	870.54
	0.5	27.54	128.15	299.98	554.46	852.19
	1	18.61	97.57	232.42	421.95	665.84
	2	12.85	74.45	179.66	327.51	517.77
SFSS	0	18.92	62.44	143.46	260.81	413.39
	0.5	11.13	54.11	134.12	255.02	400.72
	1	5.739	39.48	102.36	193.23	311.51
	2	2.81	29.12	78.11	149.07	241.34

Numbers in parenthesis indicate the critical buckling mode.

8. APPENDIX A

The characteristic equations for various boundary conditions are

Case 1. SSSS plate

Case 2. SCSC plate

$$(2\bar{D}\lambda_1\gamma + \sqrt{\bar{D}}N_T \sinh(\lambda_1 b) \sinh(\lambda_2 b) - 2\bar{D}\gamma \cosh(\lambda_1 b)\lambda_1 \cosh(\lambda_2 b))/\sqrt{\bar{D}^3} = 0$$

Case 3. SCSS plate

$$(2\bar{D}\lambda_1^2\gamma \sinh(\lambda_1 b) \cosh(\lambda_2 b) - \gamma \sinh(\lambda_1 b) \cosh(\lambda_2 b)N_T - 2\sqrt{\bar{D}^3} \sinh(\lambda_2 b) \cosh(\lambda_1 b) + \sqrt{\bar{D}} \sinh(\lambda_2 b) \cosh(\lambda_1 b)N_T)/\sqrt{\bar{D}} = 0$$

Case 4. SFSF plate

$$\lambda_1^2 \{ (-32C^4\bar{D}\lambda_1^7\gamma + 16C^2\bar{D}^3\lambda_1^5\gamma N_T - 8C^2\bar{D}^2\lambda_1^3\gamma N_T^2 - 32C^3\bar{D}^2\lambda_1^5\gamma N_T + 32C^2\sqrt{\bar{D}^3}\lambda_1^7\gamma - 32C^2\sqrt{\bar{D}^2}\lambda_1^5\gamma N_T + 16C\bar{D}^4\lambda_1^5\gamma N_T - 16C\bar{D}^3\lambda_1^3\gamma N_T^2 + 8C^2\bar{D}\lambda_1^3\gamma N_T^2 + 4C\bar{D}^2\lambda_1\gamma N_T^3 + 8C\bar{D}^4\lambda_1^3\gamma N_T^2 - 4C\bar{D}^3\lambda_1\gamma N_T^3 - 8C^2\bar{D}^3\lambda_1^3\gamma N_T^2) \cosh(\lambda_1 b) \cosh(\lambda_2 b) + \{ 16C\sqrt{\bar{D}^9}\lambda_1^6 N_T - 16C\sqrt{\bar{D}^7}\lambda_1^4 N_T^2 + \sqrt{\bar{D}^7} N_T^4 + 4C^1\sqrt{\bar{D}^5}\lambda_1^2 N_T^3 + 4\sqrt{\bar{D}^{11}}\lambda_1^4 N_T^2 - 4\sqrt{\bar{D}^9}\lambda_1^2 N_T^3 - 8C\sqrt{\bar{D}^9}\lambda_1^4 N_T^2 + 4C\sqrt{\bar{D}^7}\lambda_1^2 N_T^3 - 64C^3\sqrt{\bar{D}^5}\lambda_1^8 + 64C^3\sqrt{\bar{D}^3}\lambda_1^6 N_T + 16C^3\sqrt{\bar{D}^3}\lambda_1^4 N_T^2 + 4C^2\sqrt{\bar{D}}\lambda_1^2 N_T^3 + 16C^4\sqrt{\bar{D}}\lambda_1^6 N_T - 16C^3\sqrt{\bar{D}}\lambda_1^4 N_T^2 + 16C^2\sqrt{\bar{D}^5}\lambda_1^6 N_T - 48C^2\sqrt{\bar{D}^7}\lambda_1^6 N_T - 16C^2\sqrt{\bar{D}^3}\lambda_1^4 N_T^2 - 8C^2\sqrt{\bar{D}^3}\lambda_1^2 N_T^3 + 4C^2\sqrt{\bar{D}^5}\lambda_1^2 N_T^3 + 40C^2\sqrt{\bar{D}^5}\lambda_1^4 N_T^2 \} \sinh(\lambda_1 b) \sinh(\lambda_2 b) + 32C^4\bar{D}\lambda_1^7\gamma - 32C^2\bar{D}^3\lambda_1^7\gamma + 4C\bar{D}^3\lambda_1\gamma N_T^3 + 8C^2\bar{D}^2\lambda_1^3\gamma N_T^2 + 8C^2\bar{D}^3\lambda_1^3\gamma N_T^2 - 16C\bar{D}^4\lambda_1^5\gamma N_T - 16C^2\bar{D}^3\lambda_1^5\gamma N_T + 16C\bar{D}^3\lambda_1^3\gamma N_T^2 - 4C\bar{D}^2\lambda_1\gamma N_T^3 + 32C^3\bar{D}^2\lambda_1^5\gamma N_T + 32C^2\bar{D}^2\lambda_1^5\gamma N_T - 8C^2\bar{D}\lambda_1^3\gamma N_T^2 - 8C\bar{D}^4\lambda_1^3\gamma N_T^2) / \sqrt{\bar{D}^3} = 0$$

Case 5. SCSF plate

$$-\lambda_1(-4C\bar{D}^2\lambda_1^2\gamma N_T + \bar{D}\gamma N_T^2 - 8C^2\bar{D}\lambda_1^4\gamma - 4\bar{D}^2\lambda_1^2\gamma N_T + 2\bar{D}^3\lambda_1^2\gamma N_T - \bar{D}^2\gamma N_T^2 + 4\bar{D}^3\lambda_1^4\gamma + \{ 8C^2\bar{D}\lambda_1^4\gamma - 2\bar{D}^3\lambda_1^2\gamma N_T + \bar{D}^2\gamma N_T^2 + 4C\bar{D}^2\lambda_1^2\gamma N_T \} \cosh(\lambda_1 b) \cosh(\lambda_2 b) + \{ -4C^2\sqrt{\bar{D}}\lambda_1^3 N_T + 2C\sqrt{\bar{D}}\lambda_1 N_T^2 + 2C\sqrt{\bar{D}^7}\lambda_1^3 N_T - 2C\sqrt{\bar{D}^3}\lambda_1 N_T^2 - \sqrt{\bar{D}^5}\lambda_1 N_T^2 + 8C\sqrt{\bar{D}^5}\lambda_1^5 - 8C\sqrt{\bar{D}^3}\lambda_1^3 N_T \} \sinh(\lambda_1 b) \sinh(\lambda_2 b)) / \sqrt{\bar{D}^3} = 0$$

Case 6. SFSS plate

$$\lambda_1 \{ (-\sqrt{\bar{D}^3} N_T^3 - 4C^2\sqrt{\bar{D}}\lambda_1^4 N_T - 2C\sqrt{\bar{D}^3}\lambda_1^2 N_T^2 - 8C\sqrt{\bar{D}^5}\lambda_1^6 + 8C\sqrt{\bar{D}^3}\lambda_1^4 N_T + 8C^2\sqrt{\bar{D}^3}\lambda_1^6 + 4\sqrt{\bar{D}^5}\lambda_1^2 N_T^2 - 4\sqrt{\bar{D}^7}\lambda_1^4 N_T - 2C\sqrt{\bar{D}}\lambda_1^2 N_T^2 + 4C\sqrt{\bar{D}^5}\lambda_1^4 N_T) \sinh(\lambda_2 b) \cosh(\lambda_1 b) + \{ -8C^2\bar{D}\lambda_1^5\gamma + 4C^2\lambda_1^3\gamma N_T - 8C\lambda_1^5\bar{D}^2\gamma + 8C\lambda_1^3\bar{D}\gamma N_T - 2C\lambda_1\gamma N_T^2 - 4C\bar{D}^2\lambda_1^3\gamma N_T + 2C\bar{D}\lambda_1\gamma N_T^2 \} \sinh(\lambda_1 b) \cosh(\lambda_2 b) \} / \sqrt{\bar{D}} = 0$$

$$\text{where } \gamma = \sqrt{N_T - \bar{D}\lambda_1^2} \text{ and } C = \frac{(1-\nu)\bar{D}}{2}.$$

9. REFERENCES

1. Koizumi, M., "FGM activities in Japan", *Compos. B*, Vol. 28, (1997), 1-4.
2. Javaheri, R. and Eslami, M.R., "Buckling of functionally graded rectangular plates under in plane compressive loading", *ZAMM*, Vol. 82, No. 4, (2002), 277-283.
3. Javaheri, R. and Eslami, M.R., "Thermal buckling of functionally graded rectangular plates", *AIAA Journal*, Vol. 40, No. 1, (2002), 162-169.
4. Javaheri, R. and Eslami, M.R., "Thermal buckling of functionally graded rectangular plates based on higher order theory", *J. Thermal Stresses*, Vol. 25, (2002), 603-625.
5. Samsam Shariat, B.A. and Eslami, M.R., "Thermal buckling of imperfect functionally graded plates", *International journal of solids and structures*, Vol. 43, (2005), 4082-4096.
6. Lanhe, W., "Thermal buckling of a simply supported moderately thick rectangular FGM plate", *Composite Structures*, Vol. 64, (2004), 211-218.
7. Wu, T.L., Shukla, K.K. and Huang, J.H., "Post buckling analysis of functionally graded rectangular plates",

- Composite Structures*, Vol. 81, (2007), 1-10.
8. Shariat, B.A.S. and Eslami, M.R., "Buckling of thick functionally graded plates under mechanical and thermal loads" *Composite Structures*, Vol. 78, (2005), 433-439.
 9. Abrate, S., "Free vibration, buckling and static deflections of functionally graded plates", *Composites Science and Technology*, Vol. 66, (2005), 2383-2394.
 10. Abrate, S., "Functionally graded plates behave like homogeneous plates", *Compos B*, Vol. 39,(2008),151-158.
 11. Liu, Y.G. and Pavlovic, M.N., "A generalized analytical approach to buckling of simply-supported rectangular plates under arbitrary loads", *Engineering Structures*, Vol. 30, (2008), 1346,1359.
 12. Matsunaga, H., "Free vibration and stability of functionally graded plates according to a 2-D higher order deformation theory", *Composite Structures*, Vol. 82, (2008), 499-512.
 13. Matsunaga H. Stress analysis of functionally graded plates subjected to thermal and mechanical loading. *Composite Structures*, Vol. 87, (2009), 344-357.
 14. Hosseini-Hashemi, S., Khorshidi, K. and Amabili, M., "Exact solution for linear buckling of rectangular Mindlin plates", *Journal of Sound and Vibration*, Vol. 315, (2008), 318-342.
 15. Mohammadi, M. Saidi, A.R. and Jomehzadeh, E. "Levy Solution for Buckling Analysis of Functionally Graded Rectangular Plates", *Appl Compos Mater*, Vol. 17, (2010), 81-93.
 16. Mirzaeifar, R., Shahab, S. and Bahai, H., "An approximate method for simultaneous modification of natural frequencies and buckling loads of thin rectangular isotropic plates", *Engineering Structure*, Vol. 31, (2009), 208-215.
 17. Saidi, A.R., Rasouli, A. and Sahraee, S., "Axisymmetric bending and buckling analysis of thick functionally graded circular plates using unconstrained third order shear deformation plate theory", *Composite Structures*, Vol. 89, (2009), 110-119.
 18. Saidi, A.R. and Jomehzadeh, E., "On analytical approach for the bending/stretching of linearly elastic functionally graded rectangular plates with two opposite edges simply supported", *IMechE part C, Journal of Mechanical Engineering science*, Vol. 223, (2009), 2009-2016.
 19. Praveen, G. N., and Reddy, J. N., "Nonlinear transient thermoelastic analysis of functionally graded ceramic-metal plates", *Int. J. Solids Structures*, Vol. 35, (1998), 4457-4476.
 20. Woo, J., and Meguid, S. A., "Nonlinear analysis of functionally graded plates and shallow shells", *Int. J. Solids Structures*, Vol. 38, (2001), 7409-7421.
 21. Jomehzadeh, E., Saidi A.R. and Atashipour S.R., "An analytical approach for stress analysis of functionally graded annular sector plates", *Materials & Design*, Vol. 30, (2009), 3679-3685.
 22. Brush D.O. and Almroth B.O. "Buckling of bars, plates, and shells". McGraw-Hill, New-York, (1975), 75-120.